

Generating and verifying graph states for fault-tolerant measurement-based quantum computing in 2D optical lattices

Jaewoo Joo

Quantum Information Science, School of Physics and Astronomy, University of Leeds,
Leeds LS2 9JT, U.K.

Emilio Alba

Instituto de Física Fundamental, Consejo Superior de Investigaciones Científicas,
Calle Serrano 113b, Madrid E-28006, Spain

Juan José García-Ripoll

Instituto de Física Fundamental, Consejo Superior de Investigaciones Científicas,
Calle Serrano 113b, Madrid E-28006, Spain

Timothy P. Spiller

Quantum Information Science, School of Physics and Astronomy, University of Leeds,
Leeds LS2 9JT, U.K.

Abstract. We propose two schemes for implementing graph states useful for fault-tolerant measurement-based quantum computation in 2D optical lattices. We show that bilayer cluster and surface code states can be created by just global single-row and controlled-Z operations. The schemes benefit from the accessibility of atom addressing on 2D optical lattices and the existence of a verification protocol which allows us to ensure the experimental feasibility of measuring the fidelity of the system against the ideal graph state. The simulation results show potential for a physical realisation toward fault-tolerant measurement-based quantum computation in the presence of defects in optical lattices.

1. Background

Measurement-based quantum computation (MBQC) has provided a new paradigm of quantum computation for a decade now[1]. The required resource is a highly entangled state (such as a graph state), initially prepared in a many-component quantum system. Graph states are quantum states associated with mathematical graphs, where vertices represent qubits and edges represent controlled-Z (CZ) gates between the qubits [2]. A two-dimensional (2D) cluster state is one of the well-known graph states [3]. To construct a 2D cluster state in a physical-space 2D square lattice system, all qubits in the lattice should be initialised in state $|+\rangle = (|0\rangle + |1\rangle)/\sqrt{2}$. A controlled-Z (CZ) operation is then performed between each qubit and its four neighbouring qubits. These operations commute, so the order is unimportant. With this state as a resource, MBQC only requires a sequence of single-qubit measurements to simulate any quantum algorithm[1, 2, 3].

Of course, a simple approach to MBQC is susceptible to errors and decoherence. For example, even if a 2D cluster state could be ideally prepared, a small error during the single-qubit measurement procedure could be propagated to other qubits in the rest of the entangled system, with the accumulated errors resulting in an incorrect outcome of the quantum computation. For practical application of MBQC against the effects of errors and decoherence, the long term goal would therefore be to perform fully fault-tolerant MBQC. The construction of logical cluster states using error-correcting codes [4] and the engineering of thermal ground states of high-spin systems [5] have been proposed as theoretical platforms for fault-tolerant MBQC. However, the realistic implementation of these approaches contains many hurdles—it would be difficult to create such complicated entanglement structures in any natural physical system. A method for performing intrinsic fault-tolerance in MBQC is to create simple 3D (as opposed to 2D) cluster states [6, 7, 8] and the first in-principle demonstration has been performed in photonic states [9]. Alternatively, it is also known that surface codes (toric codes of Kitaev [10]) provide the known highest error threshold for universal fault-tolerant quantum computation [6, 11] and that a practical approach has been very recently investigated for creating multi-partite entangled states in surface code lattices [12].

Optical lattices offer advantage for building graph states due to the ability to perform global two-qubit entangling interactions, enabling many commuting operations to be performed simultaneously throughout the lattice. In particular, controlled collisions [13] and engineered interaction [14, 15, 16] provide excellent examples of desired interactions that can be manipulated globally across a lattice. Very recently, it has been demonstrated that ultra-cold lithium (Li) and caesium (Cs) atoms can be arranged to occupy every site in 2D triangular optical lattices, using diffraction masks [14]. For example, once the wave-packet of Cs is overlapped to that of Li, the qubit states can be coupled to the Li-Cs molecular state and interactions between these levels can provide the capability of two-qubit operations. The resultant operation is equivalent to

CZ gates, $U_{CZ} = \exp\left(-i\frac{\pi}{4}\sigma_{Li}^z\sigma_{Cs}^z\right)$, up to local unitary operations (σ^i is a Pauli operator) [16].

Although direct individual single-atom addressing in 2D optical lattices is still challenging in experiments to perform MBQC [17], due to the comparable wavelengths of trapping and addressing lasers, significant experimental progress has been made towards single-atom addressing (e.g., using pointer atoms, laser interference patterns, microwave transitions, etc.) [18, 19, 20, 21, 22]. For example, a Hadamard operation on an atom given by $H = (\sigma^x + \sigma^z)/\sqrt{2}$ can be performed globally by microwave transitions between $|0\rangle$ and $|1\rangle$, or applied magnetic fields over sites [21]. Note that no single-site addressing is required to prepare graph states in bipartite lattice systems.

Despite the promise of optical lattices, significant issues exist for the implementation of resource states toward fault-tolerant MBQC. It is very difficult and slow to check and verify the entanglement of prepared graph states [23], when relying on individual qubit addressing. To tackle this issue, we provide efficient verification schemes based on global single-qubit measurements. Another issue is the construction of a 3D atomic cluster state in a 3D *spatial* optical lattice system. This has a significant hurdle because of the site access problems and lack of single-atom addressability. To tackle this issue, we provide a method to embed a 3D logical structure in a 2D physical structure. At this point it is appropriate to draw a clear distinction between the spatial dimensionality of the the lattice system in real physical space and the effective spatial dimension of the quantum resource constructed. Although it is often the case that these are one in the same, it is not always so.

2. Two schemes

We now present two theoretical implementation schemes that provide potential for fault-tolerant MBQC built upon 2D optical lattices. In scheme (i) we demonstrate how to construct 3D (in state space) cluster states in a spatially 2D lattices. In scheme (ii) we demonstrate how to construct 2D graph states on the surface code. Both schemes share the same experimental set-up: two inter-penetrating optical lattices, with either rectangular or square geometry, which combine to form a square lattice. Each sub-lattice confines a different atomic species in a Mott insulating state such as Cs and Li denoted with different colours in figures. The construction protocols for both states rely on the same ingredients: nearest-neighbour CZ two-qubit gates and a patterned set of Hadamard gates used to prepare qubits in $|0\rangle$ and $|+\rangle$ states (empty and solid circles in Figs. 1 and 2). The set of CZ gates is achieved by means of controlled collisions between the two sub-lattices [14]. The two atomic species can be displaced relative to each other [14], performing the nearest-neighbour two-qubit gates. For the patterned Hadamard, one might rely on single-site addressing [20], but the result would be prone to decoherence due to slow operation time. Another possibility is to apply two Raman lasers on a standing wave configuration whose period doubles that of the individual sub-lattices. Acting solely on the “red” sites, this lattice would implement a Hadamard

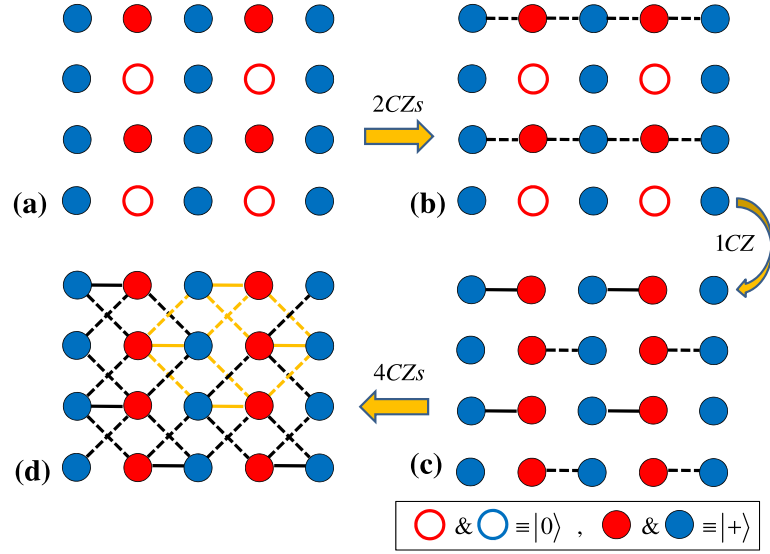


Figure 1. To build 3D cluster states, 7 CZ and 2 hadamard operations are globally required in 2D optical lattices. Dashed lines indicate CZ operations at the stage while solid lines do in the previous stages. In (d), the coloured edges present a unit cell of 3D cluster states in the lattices.

gate on the k -th row, creating an alternation between $|0\rangle$ and $|+\rangle$ states. It is also possible to achieve single-row resolution in order to create a magnetic field gradient which implements a $R_z(k\pi) = \exp[-i\frac{k\pi}{2}\sigma^z]$ rotation every second row of one atomic species. Combined with two global rotations, $H_{pseu} \propto R_y(\pi/4)R_z(k\pi)R_y(\pi/4)$, this creates the desired gate pattern [24]. In a final stage the two species can be independently imaged with single site resolution [20].

2.1. Scheme (i): 3D cluster states

The first implementation scheme, for building a bilayer (effective) 3D cluster state, is inspired by Ref. [25]. The construction of the cluster state in (spatial) 2D optical lattices requires 7 global CZ operations overall, along with the patterned Hadamard operations already described. However, in contrast to the ion trap scheme, we provide a verification protocol that is a simple but powerful tool to check the multipartite entanglement that should exist in a 3D cluster state constructed in a 2D atomic lattice. The detailed operational sequence is depicted in Fig. 1. The starting point is the set of optical lattices in the patterned states of two species indicated in Fig. 1(a). Once the 1D cluster states are made by 2 global CZ operations (see Fig. 1(b)), an additional patterned Hadamard operation is then performed at every second row of Li atoms. Then, an additional global CZ operation (e.g., CZ from red to blue) is performed to obtain the pair-wise patterned entangled state as shown in Fig. 1(c). Finally, we perform CZ operations in four diagonal directions. The final outcome is equal to a 3D cluster states in a 2D optical lattice system, as shown in Fig. 1(d). Due to the proposed structure based on physically 2D optical lattices, our scheme provides a measurement

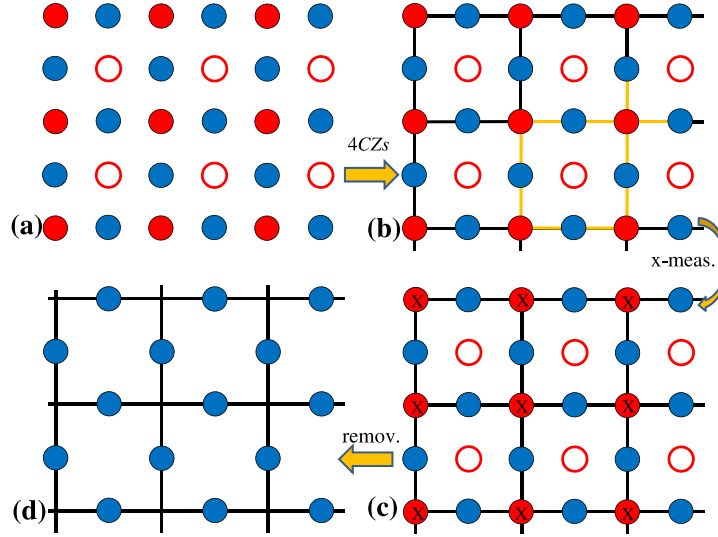


Figure 2. How to build a surface code in 2D optical lattices. The surface code is created by local σ^x measurements (denoted by X) from a 2D cluster state in (c) [6]. Then, Li atoms are removed by turning off their optical lattices.

capability for the full atomic 3D cluster state, with lasers directed from the third spatial dimension (orthogonal to the 2D lattice). In principle, the layers in the 3D cluster could be extended in state space by adding different species of atoms in 2D physical space.

2.2. Scheme (ii): surface code states

In our second implementation scheme, we demonstrate that the surface code can be created by local σ^x measurements from a graph (2D cluster-like) state. It is even more economical (in terms of global gates) to build a quantum state that embeds the surface code. The patterned state is the initialised state as shown in Fig. 2(a). After four CZ operations (two horizontal and two vertical) are performed between Li and Cs atoms (some Li atoms are in state $|0\rangle$), the intermediate state has patterned entanglement as shown in Fig. 2(b) and is used for performing a verification protocol. Taking the advantage of the interlocking optical lattices, we globally perform σ^x measurements on all Li atoms and the measurement outcomes provide us the information of existing anyons in optical lattices [12]. In addition, if single-site readout is feasible, the result of the σ^x measurements could be also used for verifying the stabilizer operators of the surface code. After this, all the Cs atoms are dropped by turning off their optical lattice. The resultant state is therefore equivalent to the surface code encoded state as shown in Fig. 2(d).

3. Simulation

We now show simulations of applying the verification protocol to the basic building blocks of our graph states in Fig. 1(d) and Fig. 2(b). Yellow lines indicate a basic

cube block for the bilayer 3D cubic cluster state in Fig. 1(d) and for the surface-code-generating graph state in Fig. 2(b).

3.1. Verification protocol

Verifying the success of the experimental protocol which creates the graph state (Fig. 1(d) and 2(b)) is a powerful tool to ensure MBQC can be performed in the designed set-up. It has been shown that the connectivity of graph states in 2D optical lattices can be verified by solely using the performance of σ^x and σ^z measurements [16]. This is so because the graph state is the eigenstate of the set of stabilizer operators $S_i = \sigma_i^x \prod_{j \in \mathcal{N}(i)} \sigma_j^z$ with eigenvalue +1, where $\mathcal{N}(i)$ stands for all nearest neighbours of the lattice site i . Therefore $P = \prod_i (1 + S_i/2)$ is a projector which directly measures the fidelity of any give state to a graph state.

A remarkable feature of the proposed schemes is that the resulting graph states are bipartite, i.e. they can be represented by a graph composed by two disjoint unconnected sets of vertices [26]. This property is enough to show that the fidelity of the experimental state to a graph state can be computed with only two sets of operators [27]. We shall denote by A and B two sets of lattice sites, which will be fixed for each of our schemes. These sets are to be complementary ($A \cup B$ is the whole lattice) and disjoint ($A \cap B = \emptyset$). It is possible to simultaneously measure σ_i^x for all $i \in A$ and σ_j^z for all $j \in B$ since all these Pauli operators commute with each other. This also holds for the simultaneous measurement of σ_i^z for all $i \in A$ and σ_j^x for all $j \in B$. These single-site measurements suffice to compute

$$\langle P_M \rangle = \left\langle \prod_{i \in M} \frac{1}{2} \left(\mathbb{1} + \sigma_i^x \prod_{j \in \mathcal{N}(i)} \sigma_j^z \right) \right\rangle \quad (1)$$

where $\mathcal{N}(i)$ stands for all nearest neighbours of i in the graph associated to the graph state ($M = A, B$). Each of the two projectors can be evaluated with a single experimental setup, and the fidelity of the system to the ideal graph state can be bounded by $\mathcal{F} \geq \langle P_A \rangle + \langle P_B \rangle - 1$ and thus needs only two experimental setups. Moreover, this protocol allows for detection of high-fidelity regions in the presence of defects [16].

3.2. Simulation results

In order to apply the verification protocol to our schemes, we only need to specify the disjoint sets A and B for each case. In the cluster state of Fig. 1(d), these sets have to be chosen as the even and odd columns (or vertical rows in the picture) of the lattice. It is remarkable that such a simple pattern works for a projection of an effective cubic lattice. The cluster state of Fig. 2(b), which is an intermediate step towards the surface code, can be verified even more easily, since the disjoint sets are the set of Li and Cs atoms. In in Fig. 3(a)-(b), shaded atoms represent the border of the unit blocks, which has to be measured to compute the local fidelity.

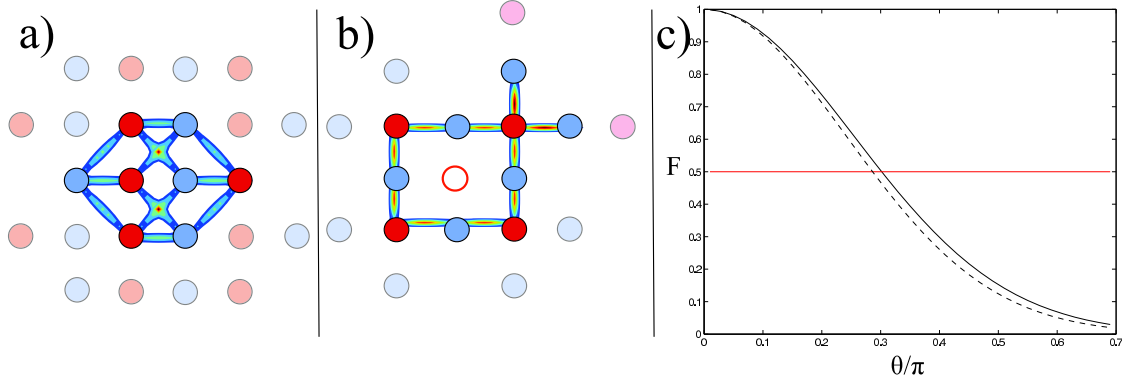


Figure 3. a-b) Simulation of the application of the 2-qubit verification protocol in the basic blocks respectively. The Ising error parameter angle is $\theta = \pi/5$. Shaded atoms represent the border of the unit blocks, which has to be measured to compute the local fidelity. c) Value of the entanglement witness as a function of θ for the cubic block (solid) and the surface-code block (dashed). The horizontal line shows the minimum value for the observable to show genuine multipartite entanglement. Notice that the graphs are roughly similar due to the similar size of the blocks considered.

Several sources of experimental error can be quantified in simulating the application of the protocol to a unit block (e.g., inaccurate qubit initialization [16], global phase errors [28]). We will focus on simulations considering that the main source of error comes from the implementation of the entangling CZ gates. This error can be parametrized by a dephasing angle θ which quantifies the deviation from the ideal pulse times or beam energies. A natural expression of this error is in terms of a unitary map acting on our qubits: $U_{CZ}^{j,k} \rightarrow U_{CZ}^{j,k} \exp(i\theta'_{j,k} \sigma_z^j \sigma_z^k)$. One example of an error distribution is to take θ' as a uniformly distributed random variable within the interval $[-\theta, \theta]$.

The results of our simulations are shown in Fig. 3(c), where we compute the bipartite bound of the local fidelity $\mathcal{F} \geq \langle P_A \rangle + \langle P_B \rangle - 1$ for our states as a function of the decoherence parameter and show a colour plot of the 2-qubit fidelity for a fixed (and moderately low) value of θ . As an example, an error parameter θ lower than $\pi/20$ is enough to obtain a fidelity above 0.98 in both models.

4. Summary and remarks

In summary, we have studied the implementation of useful graph states for fault-tolerant MBQC in optical lattices. Only a global single-row and CZ operations are required to build the two graph states (bilayer cluster and surface code states). This implementation approach has three main features. First, we propose to take advantage of and utilise a practical approach for the creation of bipartite graph states, that has recently been demonstrated in experiments with optical lattices [14]. Second, the implementation scheme of 3D clusters offers us atomic addressability because bilayer cluster states can be constructed within the geometry of 2D optical lattices. Finally, compared with

other systems, the bipartite graph states in 2D optical lattices provide a unique and efficient verification protocol, to guarantee the fidelity of the resulting states before the performance of fault-tolerant MBQC. The proposed schemes could therefore be useful for a practical approach in not only quantum computation, but also quantum memory [12].

In order to perform full fault-tolerant MBQC in 2D optical lattices, there is still a long way to go. Individual single-qubit measurements need to be performed very accurately in 2D optical lattices. The fidelity between ideal and prepared graph states must overcome error-thresholds in each implementation scheme [6, 11]. Atom losses (or vacancies in optical lattices) could result in undesirable graph states and a simple source of errors could come from inaccurate qubit initialization [16].

5. Acknowledgements

We acknowledge J. K. Pachos for useful discussions and financial support from the European Commission of the European Union under the FP7 Integrated Project Q-ESSENCE, the Spanish MICINN Project FIS2009-10061, FPU No.AP 2009-1761 and CAM research consortium QUITEMAD S2009-ESP-1594.

6. Reference

- [1] Raussendorf R and Briegel H J 2001 *Phys. Rev. Lett.* **86** 5188
Raussendorf R, Browne D E and Briegel 2003 *Phys. Rev. A* **68** 022312
- [2] Hein M, Eisert J and Briegel H J 2004 *Phys. Rev. A* **69** 062311
Van den Nest M, Dehaene J and DeMoor B 2004 *Phys. Rev. A* **69** 022316
- [3] Briegel H J and Raussendorf R 2001 *Phys. Rev. Lett.* **86** 910
- [4] Joo J and Feder D L 2011 *New. J. Phys.* **13** 063025
Fujii K and Yamamoto K 2010 *Phys. Rev. A* **82** 060301(R)
Joo J and Feder D L 2009 *Phys. Rev. A* **80** 032312
- [5] Li Y, Browne D E, Kwek L C, Raussendorf R and Wei T-C 2011 *Phys. Rev. Lett.* **107** 060501
Wei T-C, Affleck I and Raussendorf R 2011 *Phys. Rev. Lett.* **106** 070501
Wei T-C, Raussendorf R and Kwek L C 2011 *Phys. Rev. A* **84** 042333
Feder D L 2012 *Phys. Rev. A* **85** 012312
- [6] Raussendorf R, Harrington J and Goyal K 2007 *New J. Phys.* **9** 199
Raussendorf R and Harrington J 2007 *Phys. Rev. Lett.* **98** 190504
Raussendorf R, Harrington J and Goyal K 2006 *Ann. Phys.* **321** 2242
- [7] Devitt S J, Stephens A M, Munro W J and Nemoto K 2011 *New J. Phys.* **13** 095001
Devitt S J, Fowler A G, Stephens A M, Greentree A D, Hollenberg L C L, Munro W J and Nemoto K 2009 *New J. Phys.* **11** 083032
Herrera-Martí D A, Fowler A G, Jennings D and Rudolph T 2010 *Phys. Rev. A* **82** 032332
- [8] Munro W J, Harrison K A, Stephens A M, Devitt S J and Nemoto K 2010 *Nat. Photonics* **4** 792
Ionicioiu R and Munro W J 2010 *Int. J. Quant. Inf.* **8** 149
- [9] Yao X-C, Wang T-X, Chen H-Z, Gao W-B, Fowler A G, Raussendorf R, Chen Z-B, Liu N-L, Lu C-Y, Deng Y-J, Chen Y-A and Pan J.-W. 2012 *Nature* **482** 489
- [10] Kitaev A 2003 *Ann. Phys. (N.Y.)* **303** 2
- [11] Barrett S D and Stace T M 2010 *Phys. Rev. Lett.* **105** 200502

- Wang D S, Fowler A G and Hollenberg L C L 2011 *Phys. Rev. A* **83** 020302
- Fowler A G, Stephens A M and Groszkowski P 2009 *Phys. Rev. A* **80** 052312
- [12] Wootton J R and Pachos J K 2011 *Phys. Rev. Lett.* **107** 030503
- Stark C, Pollet L, Imamoglu A and Renner R 2011 *Phys. Rev. Lett.* **107** 030504
- Horsman C, Fowler A G, Devitt S and Van Meter R arXiv:1111.4022
- [13] Jaksch D, Bruder C, Cirac J I, Gardiner C W and Zoller P 1998 *Phys. Rev. Lett.* **81** 3108
- Büchler H P, Blatter G and Zwerger W 2003 *Phys. Rev. Lett.* **90** 130401
- Greiner M, Mandel O, Esslinger T, Hänsch T W and Bloch I 2002 *Nature* **415** 39
- [14] Soderberg K-A B, Gemelke N and Chin C 2009 *New J. Phys.* **11** 055022
- Klinger A, Degenkolb S, Gemelke N, Soderberg K-A B and Chin C 2010 *Rev. Sci. Instrum.* **81** 013109
- [15] Kuznetsova E, Bragdon T, Côté R, and Yelin S F 2012 *Phys. Rev. A* **85** 012328
- [16] Alba E, Tóth G and García-Ripoll J J 2010 *Phys. Rev. A* **82** 062321
- [17] Bloch I 2008 *Nature* **453** 1016
- [18] You L and Chapman M S 2000 *Phys. Rev. A* **62** 052302
- Calarco T, Dorner U, Julienne P S, Williams C J and Zoller P 2004 *Phys. Rev. A* **70** 012306
- [19] Joo J, Lim Y L, Beige A and Knight P L 2006 *Phys. Rev. A* **74** 042344
- Cho J 2007 *Phys. Rev. Lett.* **99** 020502
- [20] Weitenberg C, Endres M, Sherson J F, Cheneau M, Schauss P, Fukuhara T, Bloch I and Kuhr S 2011 *Nature* **471** 319
- Sherson J F, Weitenberg C, Endres M, Cheneau M, Bloch I and Kuhr S 2010 *Nature* **467** 68.
- [21] Mintert F and Wunderlich C 2001 *Phys. Rev. Lett.* **87** 257904
- Schrader D, Dotsenko I, Khudaverdyan M, Miroshnychenko Y, Rauschenbeutel A and Meschede D 2004 *Phys. Rev. Lett.* **93** 150501
- Zhang C, Rolston S L and Das Sarma S 2006 *Phys. Rev. A* **74** 042316
- Johanning M, Braun A, Timoney N, Elman V, Neuhauser W and Wunderlich Ch 2009 *Phys. Rev. Lett.* **102** 073004
- [22] Ospelkaus C, Warring U, Colombe Y, Brown K R, Amini J M, Leibfried D and Wineland D J 2011 *Nature* **476** 181
- Timoney N, Baumgart I, Johanning M, Varón A F, Plenio M B, Retzker A and Wunderlich Ch 2011 *Nature* **476** 185
- [23] Wunderlich H, Vallone G, Mataloni P and Plenio M B 2011 *New J. Phys.* **13** 033033
- [24] Dür W, Raussendorf R, Kendon V M and Briegel H J 2002 *Phys. Rev. A* **66** 052319
- [25] Stock R and James D F V 2009 *Phys. Rev. Lett.* **102** 170501
- [26] Hein M, Dür W, Eisert J, Raussendorf R, van der Nest M and Briegel H B arXiv:quant-ph/0602096
- [27] Gühne O and Tóth G 2009 *Physics Reports* **474** 1
- [28] Garrett M C and Feder D L 2008 *New J. Phys.* **10** 033009